

Automated Aerodynamic Design Optimization System for SST Wing-Body Configuration

Daisuke Sasaki, Guowei Yang and Shigeru Obayashi (Tohoku University)

Abstract

In this research, multiobjective optimization system has been developed to reduce the aerodynamic drag and the sonic boom for SST wing-body configuration. Wing and fuselage are defined by 131 design variables and optimized at the same time. Structured multiblock grids around SST wing-body configuration are generated automatically and an Euler solver is used to evaluate the aerodynamic performance of SST wing-body configuration.

1. Introduction

One of critical tradeoffs in designing a next generation Supersonic Transport (SST) still remains between high aerodynamic efficiency for an economic flight and low sonic boom for an environmental issue. A conventional design technique is known to allow the reduction of sonic boom at the cost of increased drag.

National Aerospace Laboratory (NAL) designed a scaled supersonic experimental airplane for NEXST-I project [1]. The plane is composed of fuselage, wing and tail. The wing is designed to achieve Natural Laminar Flow over wing and the fuselage is designed based on the area rule. The resulting wing-body configuration has good aerodynamic performance. To account for the low boom, the body is then modified to have the non-axisymmetric cross section for NEXST-II project [2]. Following their work, this paper considers simultaneous optimization of wing and fuselage configurations with non-axisymmetric body. Three-dimensional wing shape is defined by its planform, warp shape and thickness distribution in total of 72 design variables [3]. 55 design variables produce non-axisymmetric fuselage configuration. Four design variables represent the wing lofting. In total, 131 design variables will define a SST wing-fuselage configuration.

To address the tradeoff, multiobjective optimization has been performed in the present optimization by using Multiobjective Genetic Algorithms (MOGAs). The present objectives are to reduce C_D at a fixed C_L as well as to satisfy the equivalent area distribution for low sonic boom proposed by Darden [4]. Multiblock grids around SST wing-body configuration are automatically generated based on the transfinite interpolation (TFI) method [5]. Multiblock Euler calculation is used to evaluate aerodynamic performance [6]. Master-slave type parallelization was performed to reduce the large computational time of each CFD evaluation in the optimization process.

2. NAL Design Competition

The present optimization is based on NAL's assignment. Design objective is to improve L/D at Mach number of 2.0 with a fixed C_L of 0.1. An optional objective is to reduce the sonic boom at Mach number of 1.6 with a fixed C_L of 0.125.

Design specification of the present SST wing-body configuration is described in Table 1. The constraints are given based on the conceptual design for SST.

3. Multiobjective Optimization

3.1 Aerodynamic Optimization

In this study, SST wing-body configurations are designed to improve the aerodynamic performance and to lower the sonic boom strength. Therefore, design objectives are to reduce C_D at Mach number 2.0 at a fixed C_L ($=0.10$) and to match Darden's equivalent area distribution that can achieve low sonic boom. To treat a complex wing-body configuration, a multiblock Euler solver is used to evaluate an aerodynamic performance. 30 blocks around a SST wing-body configuration are used for the calculation as shown in Fig. 1. This Euler solver employs total-variation-diminishing type upwind differencing and the lower-upper factored symmetric Gauss-Seidel scheme [7]. An equivalent area distribution can be calculated by the summation of equivalent cross sectional distribution and lift distribution as shown in Fig. 2. Figure 2 also shows Darden's equivalent area distribution for 300 ft fuselage SST at Mach number 1.6 at $C_L = 0.125$.

These two design objectives were optimized by the real-coded MOGA [8]. Figure 3 shows the flowchart of MOGA. The master-slave approach was taken for parallel processing of MOGA on SGI ORIGIN2000 at the Institute of Fluid Science, Tohoku University. The master PE manages MOGA, while the slave PE's compute the multiblock Euler code for each individual. The population size was set to 64 so that the process was parallelized with 32-64 PE's depending on the availability. It should be noted that the parallelization was almost 100% because of the Euler computations dominated the CPU time.

3.2 Automated CFD Evaluation

For MOGA, CFD evaluation has to be automatically performed for a given SST wing-body configuration. Figure 4 shows the flowchart of automated CFD evaluation from the given design variables.

3.2.1 Geometry Definition

Design variables are composed of three groups: wing shape, fuselage configuration and wing lofting. Design variables for the wing shape is categorized to planform, warp shape and thickness distribution. The warp shape is composed of camber and twist distributions. Figure 5 shows the definition of the planform shape based on 6 design variables: inboard and outboard spanwise lengths, chordwise lengths at kink and tip, inboard average structural sweepback angle and outboard trailing-edge sweepback angle. Bézier surfaces and B-Spline are used to represent camber, twist and thickness distributions. Fuselage configuration is defined by a Bézier surface with 37 polygons to represent complex non-axisymmetric configuration. 37 polygons correspond to 55 design variables after imposing geometric constraints to the fuselage. Four design variables are used for the wing lofting that indicates how to combine wing and fuselage. Design variables are incidence, location of extended wing root and dihedral. The total number of design variables is 131.

To generate a surface grid, a junction line between wing and fuselage has to be extracted efficiently. For this purpose, structured grids for wing and fuselage are separately generated at first (Fig. 6 (a)). The grid lines on fuselage surface that intersect the wing surface are then searched efficiently by Lawson's search [9] and they give the junction line (Fig. 6 (b)). According to the junction line, eight surface patches on the wing-body configuration are determined for the generation of multiblock grids (Fig. 6 (c)).

3.2.2 Grid Generation

From the surface patches determined above, block boundaries are easily defined for the volume grid generation. Figure 6 (d) shows the generated surface grid on wing and fuselage, respectively. Finally, volume grid can be generated by TFI method. Figure 1 shows the resulting 30 block grids around the SST wing-body configuration. Figure 7 shows sample wing-body configurations and the corresponding surface grids.

4. Results

The present optimization was performed for 20 generations and the resulting non-dominated solutions were considered as Pareto solutions. In Fig. 8, non-dominated solutions in the initial, 10th, and 20th populations are shown. In the figure, the vertical axis is the difference of equivalent area distribution from Darden's distribution. If the difference is small, then it indicates a theoretically low boom design. The Pareto front obtained from the 20th population represents the tradeoff between drag and boom. Several wing-body configurations of the Pareto solutions are also presented in the figure. In case of the initial designs, comparatively various kinds of wing-body

configuration were generated. On the other hand, the final Pareto solutions have similar wing planforms.

Three Pareto solutions are chosen for comparison: the lowest drag (LD), the lowest boom (LB) and the center of Pareto solutions (CP). Table 2 shows their aerodynamic performances and design features. In addition, their planforms and the side views of their fuselages are shown in Fig. 9. Their planform shapes appear similar because the constraint on the wing volume is very severe and thus the planform is not allowed to change drastically. On the contrary, fuselage shapes are found to have a variety. Solutions LB and CP have a similar low boom strength in contrast to solution LD. As shown in Fig. 10, LB and CP have similar distributions to Darden's especially in the fore body by getting thicker. In contrast, LD's distribution is totally different from Darden's and the fuselage shape appears thinner.

Although LD has the highest L/D of the three, its value does not appear excellent. To improve L/D more, fuselage configurations must be more slender than those of the present solutions. This indicates that MOGA has to search solutions near the geometric constraints on the fuselage. However, the present MOGA did not focus in such a region, and the solutions tend to have a thick fuselage. The present constraints on the wing and fuselage are too severe for MOGA to find a good design candidate at the edge of the feasible region. For realistic design, MOGA has to have better constraint handling. Solution LB suggests having the increased fuselage volume for the low boom at the cost of the increased drag. It indicates that, if the fuselage volume is constrained to the original size for aerodynamic efficiency, there is no way to match Darden's distribution under the present constraints on the wing. The present result therefore suggests that the lifting surface should be distributed along the fuselage for low boom and low drag. The low boom supersonic aircraft should have an innovative planform shape.

5. Conclusion

Design optimization for SST wing-body configurations was performed based on NAL design competition. Design objectives were to improve aerodynamic performance at Mach number 2.0 and to reduce sonic boom at Mach number 1.6. These two objectives were optimized by using MOGA. To evaluate an aerodynamic performance, an Euler calculation was used. The sonic boom was evaluated according to Darden's distribution. Each evaluation was parallelized on SGI ORIGIN2000 at the Institute of Fluid Science, Tohoku University.

Multiblock grid was used to treat a complex geometry of SST wing-body configuration. Geometry is defined by in total of 131 design variables. Based on these design variables, multiblock grids were automatically generated around SST

wing-body configuration by Lawson’s search and TFI method.

As a result of the optimization, 8 Pareto solutions were obtained. Three Pareto solutions were chosen for comparison. They have a variety of fuselage configurations, but a similar planform for wing shapes. Because a similar wing planform leads to a similar lift distribution, the fore body has to become thick to match Darden’s distribution for low boom. Thus, the low boom optimization simply resulted in a thick fuselage with poor aerodynamic performance. The present result suggests that a lifting surface should be distributed innovatively to reduce both boom and drag, which will result in unconventional wing-fuselage configurations. In addition, to improve the aerodynamic performance further, MOGA has to focus in the boundary of geometric constraints more. The constraint handling in MOGA remains for future research.

Table 1 Target SST wing-body specification

- **Design objective**
 - Reduction of drag (M2.0)
- **Design specification**
 - Body length ≈ 300 ft
 - Body volume $\geq 30,000$ ft³
 - Minimum diameter ≥ 11.8 ft ($0.23 \leq x/L \leq 0.70$)
 - Wing area $\approx 9,000$ ft²
 - Wing volume $\geq 16,700$ ft³
 - Maximize t/c (extended root) $\geq 4\%$
 - (other section) $\geq 3\%$
 - Taper ratio ≈ 0.1
 - T.E. sweep angle (outboard) $\leq 30.0^\circ$
 - Average structural sweep angle $\leq 48.0^\circ$
- **Option**
 - Low boom configuration (M1.6)

Table 2 Aerodynamic performances and design specifications of selected Pareto solutions

	LD	CP	LB	constraints
L/D	11.1	10.2	8.06	
Difference of Ae(t)	6569	3747	3428	
Wing Volume (ft3)	18397	18655	17441	16800
Aspect Ratio	2.073	1.937	1.799	
Taper Ratio	0.129	0.103	0.103	
Fuselage Volume (ft3)	43798	52340	62085	30000
Min. Diameter (ft)	11.97	13.03	15.74	11.8

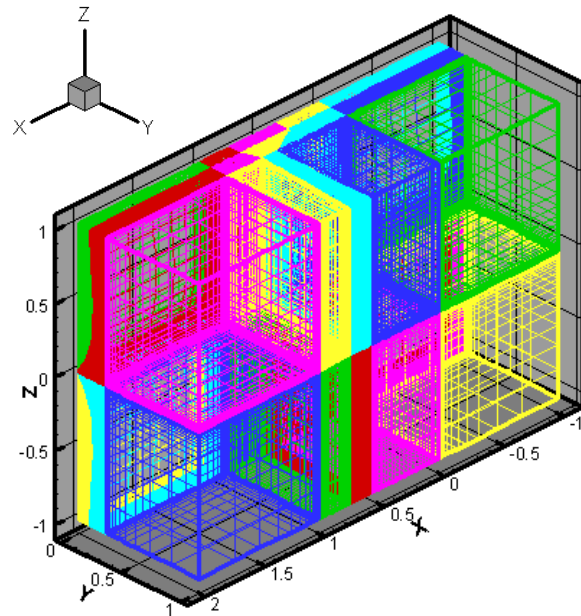


Fig. 1 30 blocks around SST wing-body configuration

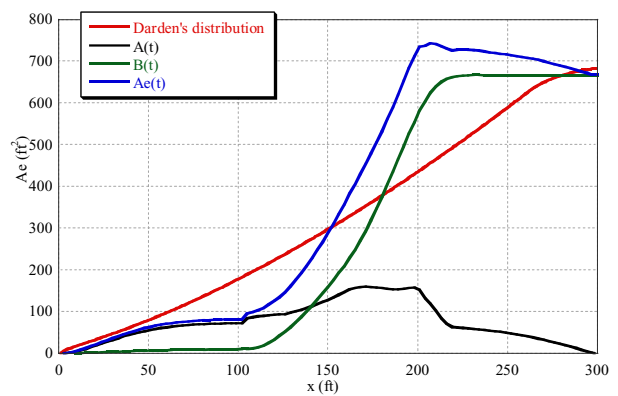


Fig.2 Equivalent area distribution of Darden's and designed geometry

Fig.3 Flowchart of MOGAs

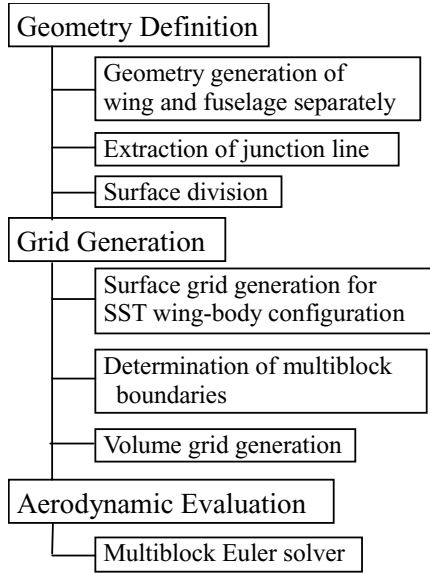


Fig.4 Flowchart of automated CFD evaluation

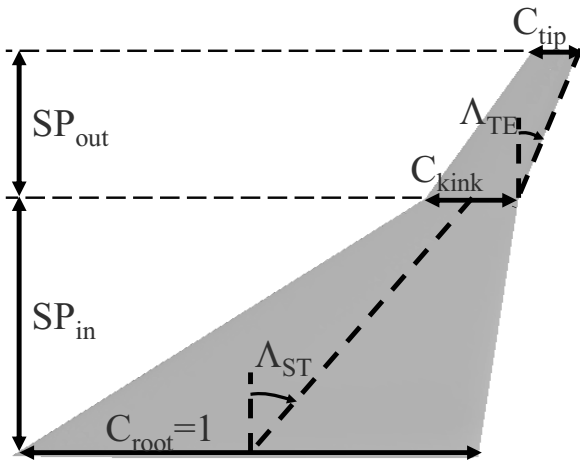
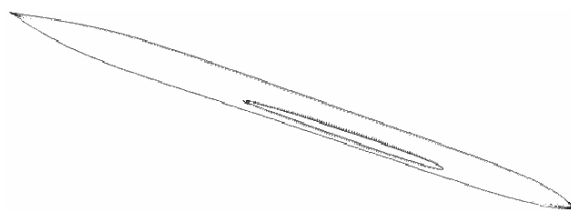
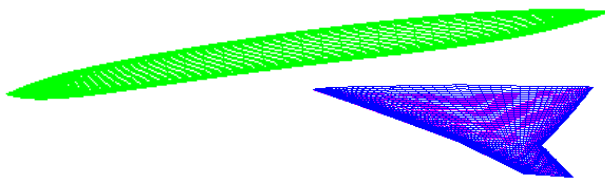
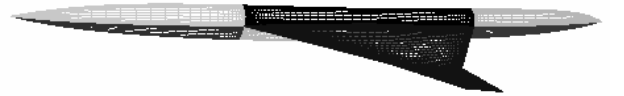


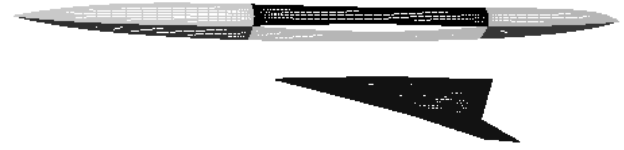
Fig.5 Planform shape definition



(b) Junction line between wing and fuselage



(c) Division of wing-body configuration



(d) Re-generated surface grid for wing and fuselage
Fig.6 Generation of surface grid on SST wing-body configuration

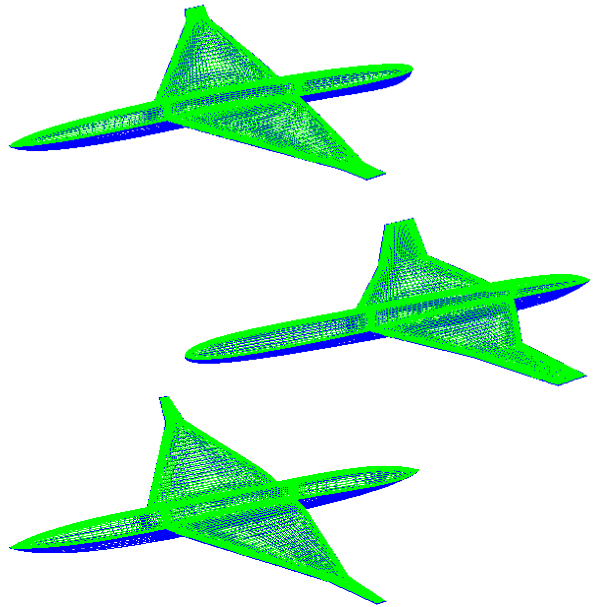


Fig. 7 Sample wing-body configurations with surface grids

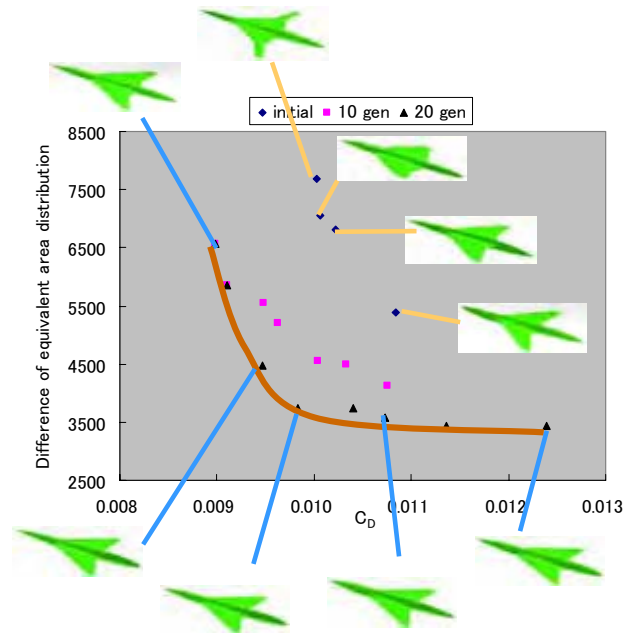
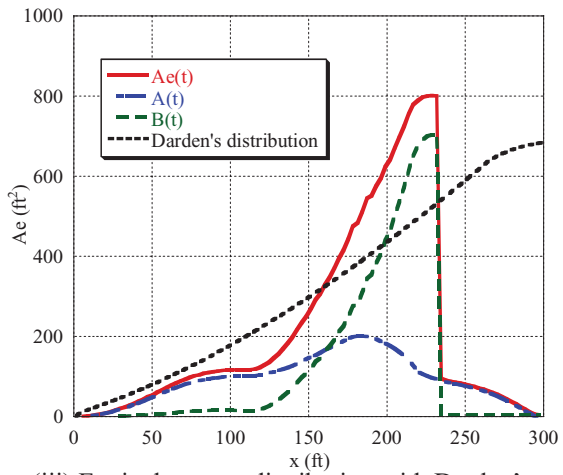
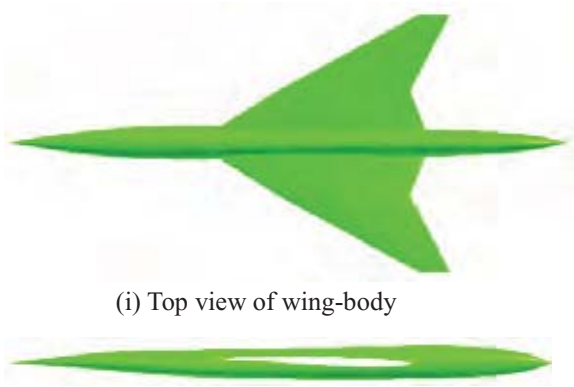
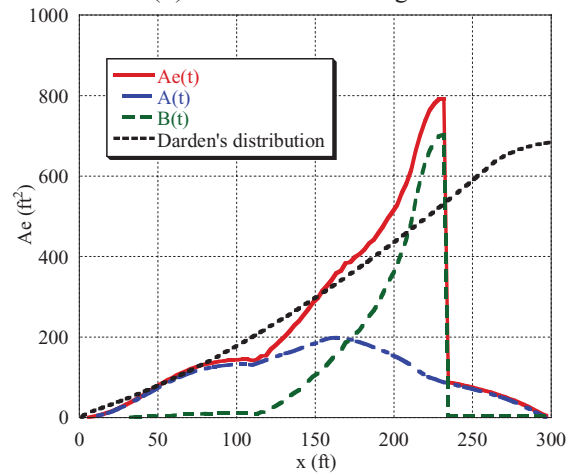
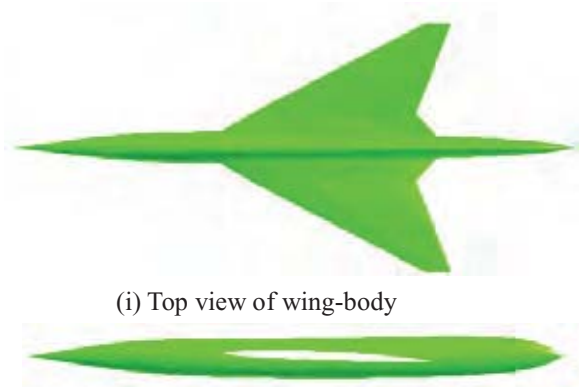


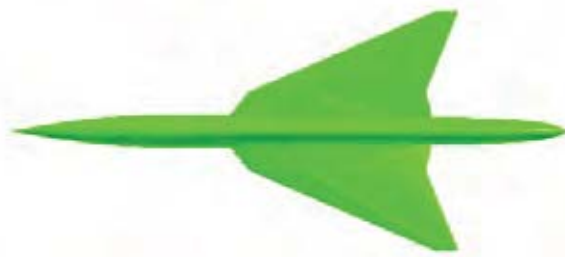
Fig.8 Pareto solutions of Initial, 10th and 20th generation with several wing-body configurations



(a) Pareto solution of highest aerodynamic performance (LD)



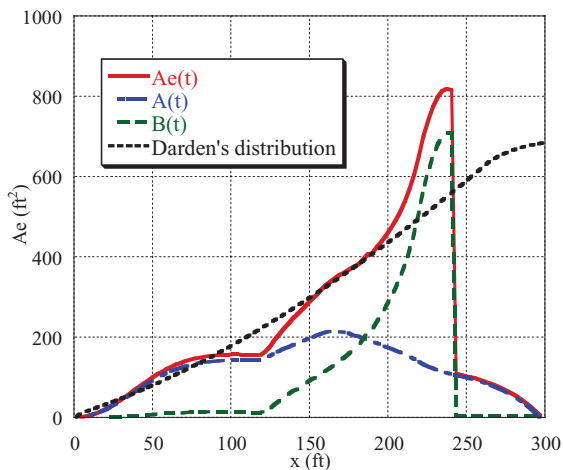
(b) Pareto solution of the center (CP)



(i) Top view of wing-body



(ii) Side view of fuselage



(iii) Equivalent area distribution with Darden's

(c) Pareto solution of lowest boom (LB)

Fig.10 Wing-body shapes and equivalent area distributions of selected Pareto solutions

Acknowledgments

The present computation was carried out in parallel using ORIGIN2000 in the Institute of Fluid Science, Tohoku University. The third author's research has been partly supported by Bombardier Aerospace, Toronto, Canada. The authors would like to thank Dr. Yoshida and NAL's SST Design Team for providing many useful data.

References

- [1] Iwamiya, T., Yoshida, K., Shimbo, Y., Makino, Y. and Matsuhima, K., "Aerodynamic Design of Supersonic Experimental Airplane," *Proc. of the 2nd SST-CFD Workshop*, pp. 79-84, 2000.
- [2] Makino, Y. and Iwamiya, T., "Aerodynamic Nacelle Shape Optimization for NAL's Experimental Airplane," *Proc. of the 2nd SST-CFD Workshop*, pp. 115-120, 2000.

- [3] Sasaki, D., Obayashi, S. and Nakahashi, K., "Navier-Stokes Optimization of Supersonic Wings with Four Objectives Using Evolutionary Algorithm," *Journal of Aircraft*, Vol. 39, No. 4, pp.621-629, 2002.
- [4] Darden, C. M., "Sonic Boom Theory: Its Status in Prediction and Minimization," *Journal of Aircraft*, Vol. 14, No. 6, pp. 569-576, 1977.
- [5] Jones, W. T., "A grid Generation System for Multi-Disciplinary Design Optimization", AIAA Paper 97-2039, 1997.
- [6] Yang, G, Kondo, M. and Obayashi, S., "Multiblock Navier-Stokes Solver for Wing/Fuselage Transport Aircraft," *JSME International Journal, Series B*, Vol. 45, No. 1, pp. 85-90, 2002.
- [7] Yoon, S. and Jameson, A., "Lower-Upper Symmetric-Gauss-Seidel Method for the Euler and Navier-Stokes Equations, *AIAA Journal*, Vol. 26, pp. 1025-1026, 1988.
- [8] Deb, K., *Multi-Objective Optimization using Evolutionary Algorithms*, John Wiley & Sons, Ltd., Chichester, 2001.
- [9] Taniguchi, T., *Automatic Element Division for FEM*, Morikita publishing house, Tokyo, 1992 (in Japanese).